HYBRID MODEL PREDICTIVE CONTROL OF THE CURRENT PROFILE IN NSTX-U
Incorporating Pulse Width Modulation Constraints Arising in Neutral Beam Injection

B. LEARD, Z. WANG, S. T. PARUCHURI, E. SCHUSTER, T. RAFIQ
Lehigh University
Bethlehem, USA
Email: brian.leard@lehigh.edu

Abstract

A novel hybrid Model Predictive Control (MPC) algorithm has been designed for simultaneous safety factor (q) profile and stored energy (W) control while incorporating the pulse-width-modulation constraints associated with the neutral beam injection system. Regulation of the q-profile has been extensively shown to be a key factor for improved confinement as well as non-inductive sustainment of the plasma current. Simultaneous control of W is necessary to prevent the triggering of pressure-driven magnetohydrodynamic instabilities as the controller shapes the q profile. Conventional MPC schemes proposed for q-profile control have considered the NBI powers as continuous-time signals, ignoring the discrete-time nature of these actuators and leading in some cases to performance loss. The hybrid MPC scheme in this work has the capability of incorporating the discrete-time actuator dynamics as additional constraints. In nonlinear simulations, the proposed hybrid MPC scheme demonstrates improved q-profile+W control performance for NSTX-U operating scenarios.

1. INTRODUCTION

Successful operation of reactor-grade tokamaks for long-pulse and steady-state scenarios requires improved plasma confinement and high non-inductive current drive fraction. Achieving these scenarios necessitates careful regulation of the safety factor (q) profile, which is closely related to the poloidal magnetic flux. As the q-profile is shaped it is important to avoid pressure-driven magnetohydrodynamic instabilities, which can be accomplished by simultaneously controlling the stored energy (W). Synchronous regulation of both the q-profile and W often requires actuation methods such as neutral beam injection (NBI). As the name implies, NBI injects high energy neutral particles into the core of the plasma. Due to their neutral charge, these particles can penetrate deep into the plasma, simultaneously adding current, heating, and torque. Consequently, NBI can be used to regulate both the magnetic and kinetic properties of the plasma, making it an effective actuator for simultaneous control of the q-profile and W. During a tokamak shot, the NBI's power level behaves in an on/off boolean style of operation. However many existing control schemes used for the safety factor profile control, such as Lyapunov control [1], optimal control [2], and robust control [3], [4], assume that the input power level is a continuous variable. This inconsistency is overcome using a continuous-to-discrete signal conversion process known as pulse-width modulation (PWM). However, in certain cases neglecting the discrete on/off actuator dynamics in the control synthesis can lead to a loss of control performance.

One control scheme that could possibly integrate the discrete nature of NBI operation is model predictive control (MPC). The MPC algorithm uses a model of the plasma dynamics to solve a real-time optimization problem that determines the optimal actuator trajectories to achieve a specific target state. One of the benefits of MPC is that it can handle time-variant actuator and state constraints. This gives it an advantage over other types of control schemes when dealing with complex systems such as tokamak plasmas. Consequently, MPC has been applied to a variety of plasma applications, from position and shape control [5], to plasma density control [6]. There have already been significant efforts to use MPC to control the safety factor profile or a related plasma property [7], [8], [9], [10], [11]. However, like many other controllers, these efforts have relied on optimization methods that assume continuous-time input and state variables. There has not been a significant effort to modify this general MPC scheme in order to incorporate the discrete-time nature of the NBI actuators and avoid the PWM conversion process. And yet, in other fields of engineering, MPC has been demonstrated to be an effective control method for similar systems. This type of MPC, known as hybrid MPC, has modified the conventional MPC algorithm to regulate systems that have both continuous-time and discrete-time components [12], [13], [14]. Hybrid MPC has been successfully employed to various applications, from self driving cars [15], to energy management for buildings [16]. There have been recent efforts to adapt this control method to density control in fusion plasma, because it is particularly suited to handle the discrete nature of pellet injection [17], [18]. However, hybrid MPC schemes have not been employed to deal with discrete NBI actuator constraints. This work seeks to use these

methods to design a hybrid MPC that incorporates the discrete-time nature of the NBI powers into the controller synthesis for simultaneous regulation of the safety factor profile and stored energy.

This paper is organized as follows. Section 2 details the control-oriented model used by the hybrid MPC to predict the evolution of the safety factor profile and stored energy. Section 3 reviews the design of a traditional MPC algorithm. Section 4 discusses the discrete constraints inherent to NBI actuators and the process of pulse-width modulation. Section 5 describes the design of the hybrid MPC. Section 6 compares the performance of the hybrid MPC to a continuous MPC in an NSTX-U scenario. Section 7 summarizes the work and discusses potential future developments.

2. CONTROL-ORIENTED MODELING OF THE POLOIDAL MAGNETIC FLUX AND STORED ENERGY

In this section, a nonlinear model of the evolution of the poloidal magnetic flux and stored energy is introduced. This model will serve as the basis for developing MPC algorithms discussed in subsequent sections.

The safety factor profile is closely related to the poloidal magnetic flux Ψ,

$$q(t,\hat{\rho}) = -\frac{d\Phi}{d\Psi} = -\frac{d\Phi}{2\pi d\psi} = -\frac{\frac{\partial\Phi}{\partial\rho}\frac{\partial\rho}{\partial\hat{\rho}}}{2\pi\frac{\partial\psi}{\partial\hat{\rho}}} = -\frac{B_{\phi,0}\rho_b^2\hat{\rho}}{\theta}, \tag{1}$$

where, Φ is the toroidal magnetic flux, $B_{\phi,0}$ represents the vacuum toroidal magnetic field at the tokamak's major radius R_0, and $\psi(t,\hat{\rho})$ is the poloidal stream function, i.e. $\psi(t,\hat{\rho}) = \Psi(t,\hat{\rho})/(2\pi)$. The variable θ is defined as the spatial gradient of the poloidal magnetic flux, $\theta \triangleq \frac{\partial\psi}{\partial\hat{\rho}}$. The symbol $\hat{\rho}$ designates the normalized mean effective minor radius, $\hat{\rho} \triangleq \rho/\rho_b$, where $\rho \triangleq \sqrt{\Phi/(B_{\phi,0}\pi)}$ is the mean effective minor radius, and ρ_b is ρ at the plasma boundary. Shown by (1), it is possible to control the evolution of the safety factor profile by controlling the spatial gradient of the poloidal magnetic flux θ.

The evolution of the poloidal magnetic flux is modeled by a one-dimensional partial differential equation (PDE) known as the magnetic diffusion equation (MDE). This equation is derived by combining Ampere's law, Faraday's law, and Ohm's law, while assuming that plasma properties are toroidally axisymmetric and constant along flux surfaces [19]. Any variable that indexes the flux coordinate can be used as a spatial coordinate. In this work, the normalized mean effective minor radius $\hat{\rho}$ is the spatial coordinate. The MDE is represented as,

$$\frac{\partial\psi}{\partial t} = \frac{\eta(T_e)}{\mu_0\rho_b^2\hat{F}^2}\frac{1}{\hat{\rho}}\frac{\partial}{\partial\hat{\rho}}\left(\hat{\rho}\hat{F}\hat{G}\hat{H}\frac{\partial\psi}{\partial\hat{\rho}}\right) + R_0\hat{H}\eta(T_e)\frac{\langle\bar{j}_{ni}\cdot\bar{B}\rangle}{B_{\phi,0}}, \qquad \frac{\partial\psi}{\partial\hat{\rho}}(t,0) = 0, \qquad \frac{\partial\psi}{\partial\hat{\rho}}(t,1) = -k_{Ip}I_p(t), \tag{2}$$

where, $\eta(t,\hat{\rho})$ is the plasma resistivity, μ_0 is the vacuum permeability, $T_e(t,\hat{\rho})$ is the electron temperature, $\bar{B}$ is the magnetic field, $\hat{F}(\hat{\rho})$, $\hat{G}(\hat{\rho})$, and $\hat{H}(\hat{\rho})$ are equilibrium parameters, $\bar{j}_{ni}(t,\hat{\rho})$ is the noninductive current drive, and $\langle\,\rangle$ denotes the flux surface average. The term k_{Ip} is a constant defined as, $k_{Ip} \triangleq \frac{-\mu_0}{2\pi}R_0\hat{G}(1)\hat{H}(1)$, and I_p is the plasma current. The noninductive current drive is composed of the current source from the actuators (in this case the NBIs) and the self-generated bootstrap current, $j_{ni} = j_{nb} + j_{bs}$. This equation is closed with a series of control-oriented models for the plasma resistivity η, the electron temperature T_e, the beam generated current j_{nb}, and the bootstrap current j_{bs}. Details on these models can be found in [20]. By incorporating these equations and taking the spatial derivative of the MDE, it is possible to obtain an equation for the evolution of the poloidal flux gradient,

$$\frac{\partial\theta}{\partial t} = \left[\frac{dC_{f_1}}{d\hat{\rho}}\theta + \left(C_{f_1} + \frac{dC_{f_2}}{d\hat{\rho}}\right)\frac{\partial\theta}{\partial\hat{\rho}} + C_{f_2}\frac{\partial^2\theta}{\partial\hat{\rho}^2}\right]\tilde{u}_{diff} + \sum_{l=1}^{L}\frac{dC_{j_l}}{d\hat{\rho}}\tilde{u}_{j_l} + \left(\frac{dC_{j_{bs}}}{d\hat{\rho}}\frac{1}{\theta} - C_{j_{bs}}\frac{1}{\theta^2}\frac{\partial\theta}{\partial\hat{\rho}}\right)\tilde{u}_{j_{bs}}, \tag{3}$$

subject to the boundary conditions $\theta(t,0) = 0$, $\theta(t,1) = -k_{Ip}I_p(t)$. In the above equation, C_{f_1}, C_{f_2}, C_{j_l} and $C_{j_{bs}}$ are functions of $\hat{\rho}$. The variables $\tilde{u}_{diff}$, $\tilde{u}_{j_l}$, and $\tilde{u}_{bs}$ are time-dependent functions of I_p, the line averaged density ($\bar{n}_e$), and the NBI powers $P_{nb,l}$, where the index l denotes the number of the NBI, with L being the total number of available NBIs. These terms are explictly defined in [21], however in this work the relationship is succinctly expressed as

$$\tilde{u} = g(u_p), \tag{4}$$

where $\tilde{u} = [\tilde{u}_{diff},\, \tilde{u}_{j1},\ldots\, \tilde{u}_{jL},\, \tilde{u}_{bs}]^T$ and $u_p = [I_p,\, \bar{n}_e,\, P_{nb,1},\ldots\, P_{nb,L}]^T$. Note that while both I_p and $\bar{n}_e$ are time varying and could be used as inputs to control the q-profile, in this work these values are prescribed by a feedforward controller, and only the NBI powers will be used for real-time feedback control.

The model in (3) is a PDE. To simplify, the model is discretized spatially using the finite difference method. Define M spatial nodes at $\hat{\rho}_m = (m-1)/(M-1)$, $m \in [1,2,\ldots M]$, where the variable θ_m denotes θ at $\hat{\rho}_m$. The

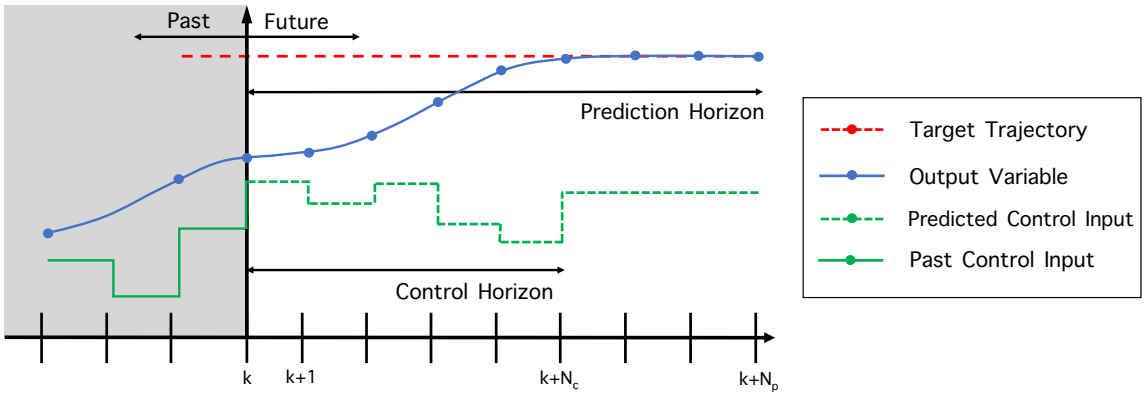

FIG. 1. Schematic showing a state and input evolution that are chosen by the MPC over a given prediction horizon.

boundary conditions are used to directly solve for the exterior nodes θ_1 and θ_M. The variable $\boldsymbol{\theta}$ is a vector containing θ_m at all interior nodes, i.e $\boldsymbol{\theta} \triangleq [\theta_2, \theta_3, \dots \theta_{M-1}]^T$. By using the finite difference approximations of derivatives, (3) is reduced from a PDE to a series of coupled ordinary differential equations (ODE's), concisely written as

$$\dot{\boldsymbol{\theta}} = f_\theta(\boldsymbol{\theta}, u), \tag{5}$$

where $u \triangleq [P_{nb,1},\ P_{nb,2}\ \dots,\ P_{nb,L}]^T$ is the input vector and the notation $\dot{(\cdot)}$ denotes a time derivative. Note that the feedforward terms I_p and $\bar{n}_e$ are assumed to be constant, rendering the above equation autonomous.

The evolution of the plasma stored energy is modeled as an ODE of the form

$$\dot{W} = -\frac{W}{\tau_e(t)} + P_{tot}(t) \triangleq f_w, \tag{6}$$

where τ_e is the energy confinement time, which is calculated based on the IPB98(y,2) scaling law found in [22]. Additionally the total power is computed as,

$$P_{tot} = \sum_{l=1}^{L} P_{nb,l} + P_{ohm} - P_{rad}, \tag{7}$$

where, P_{ohm} is the ohmic power, and P_{rad} is the radiated power. By combining the discretized poloidal flux gradient states and the total energy into a single vector, $Z = [\theta_2,\ \theta_3,\ \dots,\ \theta_{M-1},\ W]$, it is possible to succinctly write (5) and (6) as

$$\dot{Z} = F(Z, u), \tag{8}$$

where $F = [f_\theta^T, f_w]^T$.

3. CONVENTIONAL MPC DESIGN

The model predictive control scheme uses finite-time optimization to achieve the desired target. As already mentioned, it is particularly suited to handle complex systems that contain time-varying constraints. The general MPC algorithm contains three subroutines: prediction, optimization, and receding horizon implementation. The prediction subroutine calculates the response of the system for a predetermined sequence of inputs over a finite time frame, referred to as the prediction horizon. The optimization subroutine iterates on the system response obtained from the prediction routine to solve a constrained optimization problem on a user-defined cost function to determine the optimal sequence of inputs over the prediction horizon. In the receding horizon subroutine, the input value corresponding to the first time step of the optimal input sequence is implemented in the system. At each time step, the MPC algorithm employs these three interconnected subroutines to approach the target state, a process illustrated in Figure 1. Note that in the figure, during the prediction subroutine the inputs are modified over a period of time known as a control horizon, which can be either equal or shorter than the prediction horizon, and then are kept constant.

The nonlinear model derived in Section 2 can be used to predict the states while implementing MPC. However, optimization using nonlinear models can be computationally expensive and therefore are often difficult to

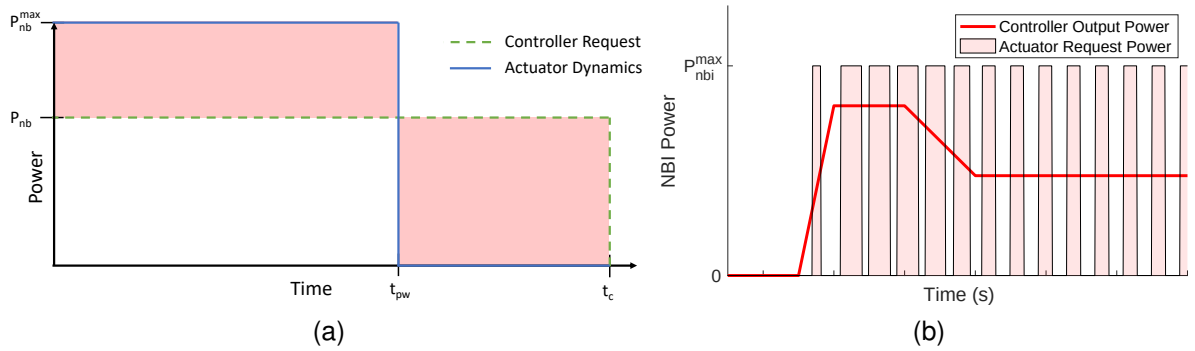

FIG. 2. Pulse-width modulation dynamics: (a) Conversion of a power request from the controller to a pulse time request for one cycle time, (b) Conversion of a continuous signal to a discrete signal over an extended time period.

implement in a real-time optimization algorithm. To reduce the computational time of the optimization process, the nonlinear system (8) can be linearized around a reference trajectory by employing first-order taylor series expansion,

$$\dot{Z} \approx F(Z_{ref}, u_{ref}) + \underbrace{\left.\frac{\partial F}{\partial Z}\right|_{Z_{ref},u_{ref}}}_{\tilde{A}} (Z - Z_{ref}) + \underbrace{\left.\frac{\partial F}{\partial u}\right|_{Z_{ref},u_{ref}}}_{\tilde{B}} (u - u_{ref}), \tag{9}$$

where u_{ref} and Z_{ref} are constant reference vectors satisfying $\dot{Z}_{ref} = F(Z_{ref}, u_{ref}) = 0$. This gives a linear time-invariant (LTI) model for the plasma dynamics. New variables $\Delta Z \triangleq Z - Z_{ref}$, and $\Delta u \triangleq u - u_{ref}$ are defined. Substituting these variables into (9) results in a linear system of the form

$$\Delta\dot{Z} = \tilde{A}\Delta Z(t) + \tilde{B}\Delta u(t). \tag{10}$$

The plasma control system for NSTX-U deals with discrete time steps. Therefore, for practical implementation, the system is discretized on a temporal grid, $t_k = k\Delta t$, $k \in [0, 1, \ldots]$, with Δt being a constant time interval. This converts the continuous-time system to

$$\Delta Z^{k+1} = A\Delta Z^k + B\Delta u^k, \tag{11}$$

where $A = \Delta t\tilde{A} + I$ and $B = \Delta t\tilde{B}$. To avoid steady-state error, the system is converted into velocity form. This is done by defining the following variables, $d\Delta Z^{k+1} = \Delta Z^{k+1} - \Delta Z^k$, and $d\Delta u^k = \Delta u^k - \Delta u^{k-1}$ and then transforming the system (11) to,

$$d\Delta Z^{k+1} = A\, d\Delta Z^k + B\, d\Delta u^k. \tag{12}$$

The fixed-horizon optimal control problem formulation can now be written as follows,

$$\min_{d\Delta u^i} \quad J = \sum_{i=k}^{N_p+k-1} (d\Delta Z^{i+1} - d\Delta Z_{tar}^{i+1})^T Q (d\Delta Z^{i+1} - d\Delta Z_{tar}^{i+1}) + (d\Delta u^i)^T R\, (d\Delta u^i) \tag{13}$$

$$\text{s.t } d\Delta Z^{i+1} = A\, d\Delta Z^i + B\, d\Delta u^i, \quad d\Delta \underline{u}^i \le d\Delta u^i \le d\Delta \bar{u}^i, \tag{14}$$

where $i = k, \ldots, N_p + k - 1$, and N_p is the number of time steps in the prediction horizon. The goal is to minimize the user defined cost function J that evaluates the deviation between the state $d\Delta Z^{i+1}$ and the target state $d\Delta Z_{tar}^{i+1}$ while simultaneously minimizing control effort. This cost function is subject to the state dynamics and each control input is bounded between a minimum $d\Delta \underline{u}^i$ and a maximum $d\Delta \bar{u}^i$, which are known as the saturation limits. Note that since these saturation limits depend on the input at the previous time-step, they are varying in time. The variables Q and R are user-defined, positive definite weighting matrices. This constrained optimization problem is solved in real-time using quadratic programming, which is overviewed in [7]. The solution to (13-14) determines the optimal inputs at a specific time step t_k.

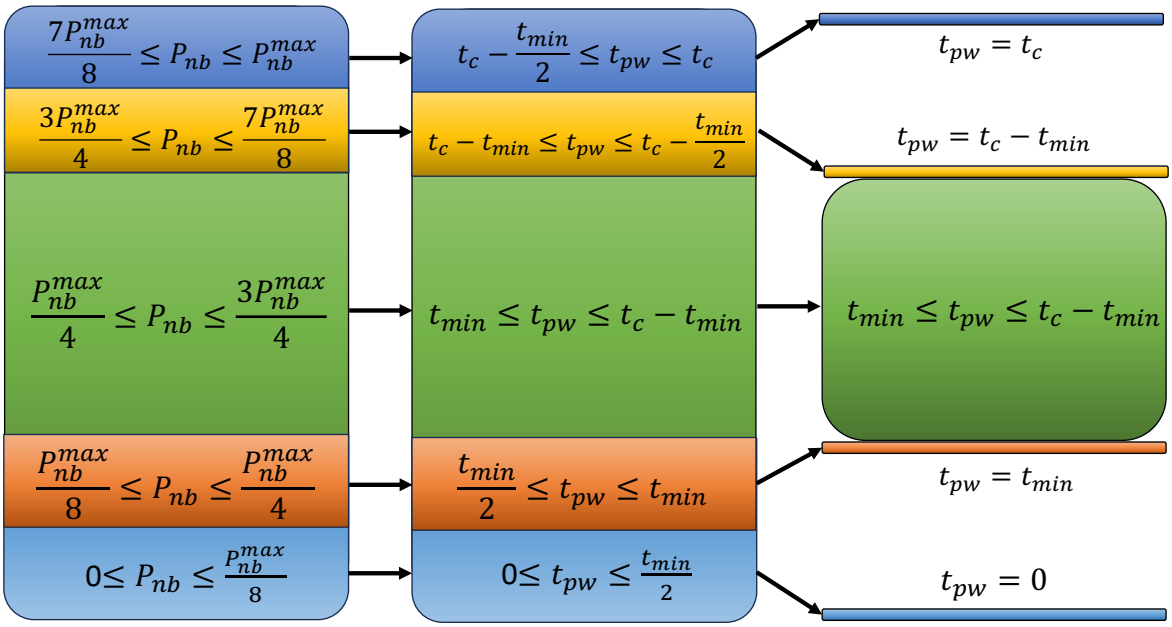

FIG. 3. The PWM filtering converts a continuous power level P_{nb} to a request time t_{pw}. However, due to mechanical constraints of NBIs, if t_{pw} falls in either the yellow and dark blue region or the orange and light blue region, it must be rounded to one of two discrete values. This introduces a piecewise nature to the range of t_{pw}.

4. PULSE-WIDTH MODULATION

While it is possible to vary the power level of an NBI by varying the supplied voltage, an NBI can only take two discrete actions, on or off, during a plasma shot. As previously stated, conventional MPC as well as other control schemes do not consider this boolean nature of NBI operation, and the conversion of continuous-time value signals from the controller to the discrete-time value signals used by the actuator is achieved by a process known as pulse width modulation. Over a prescribed time interval known as a cycling time (t_c), the NBI actuator is turned on for a period of time within this interval (called the pulse width request time (t_{pw})) and turned off for the remaining time. This is done in a way so that the average power within the cycling time equals the power level requested by the controller. In this way, PWM converts a power level request into a time request for a power pulse,

$$t_{pw} = \frac{P_{nb}\, t_c}{P_{nb}^{max}}, \tag{15}$$

where P_{nb} is the requested power by the controller and P_{nb}^{max} is the constant operational power level of the NBI. Figure 2 shows the conversion of a continuous signal to a discrete signal through PWM. Note that, due to mechanical limitations of the NBIs, t_{pw} can not take any value between 0 and t_c. There are minimum on and off times (t_{min}^{on}, t_{min}^{off}) for each NBI actuator, which limit the domain of t_{pw}. Therefore, the request time is subject to the piecewise dynamics shown in Figure 3. In this work, the minimum on and off times are assumed to be equal to one-fourth of the cycle time,

$$t_{min} \triangleq t_{min}^{on} = t_{min}^{off} = \frac{t_c}{4}. \tag{16}$$

Due to the PWM conversion as well as the restricted range of the request time due to t_{min}, there can be a significant deviation between the power waveform requested by the controller and the power waveform of the actuator. In some cases this can lead to reduced control effectiveness. Therefore, avoiding this PWM conversion process by modifying the MPC algorithm into a hybrid MPC could potentially improve overall performance of the controller.

5. HYBRID MPC DESIGN

The hybrid MPC scheme works similarly to the conventional MPC scheme, with the addition of discrete constraints that correspond to the NBI actuator limitations. However, the inclusion of these constraints necessitates the modification of the online optimization method. The model (11) is used to design the hybrid MPC. However,

in this case, at a specific time step, each component Δu_l^k, for $l = 1,\ldots,L$, in the input vector Δu^k can take only one of two values, i.e.,

$$\Delta u_l^k \in \{0 - u_{ref,l}, P_{nb}^{max} - u_{ref,l}\}, \tag{17}$$

where $u_{ref,l}$ represents the l^{th} value in the reference input vector u_{ref}. This input restriction imposes significant limitations on the controller versatility, potentially reducing the possible target trajectories achievable by the controller. However, this restriction can be utilized by the control scheme to reduce the computational effort during the optimization. Now, instead of a region of continuous input variables possible at each time step, only two possible values exist at each time step that require evaluation.

As previously discussed, along with the boolean operation of the inputs there is a minimum time an actuator must remain on or off. Since the inputs to our equation is the NBI power level and not the request time, this minimum time can be formulated as a constraint that depends on the previous values of the inputs. This requires the controller to have memory of the previous inputs to the system. Specifically, the controller must have knowledge of t_l^{sw}, which is defined as the last time step where the controller switched the l^{th} NBI on or off. Before optimizing the inputs, the controller checks the condition $t_k - t_l^{sw} < t_{min}^{on/off}$ for each NBI. If the condition is valid, then the controller assigns the input $\Delta u_l^k = \Delta u_l^{k-1}$, and Δu_l^k is removed from the optimization problem at time step t_k. Otherwise, the NBI input is incorporated into the finite-horizon optimal control problem, which can be formulated as follows,

$$\min_{\Delta u^i} \quad J = \sum_{i=k}^{N_p+k-1} (\Delta Z^{i+1} - \Delta Z_{tar}^{i+1})^T Q (\Delta Z^{i+1} - \Delta Z_{tar}^{i+1}) + (\Delta u^i)^T R (\Delta u^i) \tag{18}$$

$$\text{s.t } \Delta Z^i = A\Delta Z^i + B\Delta u^i, \tag{19}$$

$$\Delta u_l^i \in \{0 - u_{ref,l}, P_{nb}^{max} - u_{ref,l}\}, \tag{20}$$

$$\text{if} \quad t_k - t_l^{sw} < t_{min}^{on/off}, \ \text{then} \ \Delta u_l^k = \Delta u_l^{k-1}. \tag{21}$$

This is similar to the traditional MPC problem formulation where a cost function (18) is minimized while constrained by the system dynamics (19). However, the inputs are now subject to a discrete constraint (20), and a constraint based on previous inputs (21). These constraints account for the discrete nature of the NBIs. Conventional optimization techniques, such as quadratic programming, cannot handle discrete variables in the system. It is possible to implement minimization techniques that incorporate both discrete and continuous variables. In this work, since all the inputs are discrete, a systemic search method was employed to identify the optimal input combinations. The prediction horizon is assumed to be less than the minimum on/off time, i.e. $t^{k+N_p} - t^k \leq t_{min}$. This is used to expedite the optimization process, since now each NBI is restricted to one on/off switch over the prediction horizon. To simplify further, the control horizon N_c is chosen to be only one time step. The result of this limitation is that the range of possible input combinations to be evaluated reduces to 2^L. At each time step, the linear model (11) was used to predict the state evolution for possible input combinations. The combination of inputs that corresponded to the lowest cost function value was implemented for that time step, and then the process was repeated at the following time step. This proved to be a simple and effective method at determining the optimal input trajectories while maintaining acceptable computation times.

6. SIMULATION TESTING IN COTSIM

The hybrid MPC was evaluated against the continuous MPC algorithm in simulation studies carried out using the Control Oriented Tokamak SIMulator (COTSIM). COTSIM combines the magnetic diffusion equation with the heat-transport equation to model the evolution of both kinetic and magnetic properties of a tokamak plasma. These simulations were run in H-mode with a fixed temperature pedestal, and the plasma equilibrium was assumed to be constant. The tests were conducted on an NSTX-U scenario based on TRANSP shot 142301K91. All six of NSTX-U's NBIs were used in this simulation. The minimum on/off time for each NBI actuator was chosen to be $t_{min} = 0.1$ seconds, and the cycle time was chosen as $t_c = 0.4$ seconds. The feedback controllers were turned on after 0.5 seconds. Figure 4 shows the safety factor and stored energy evolutions for the simulation, and Figure 5 shows a selection of actuator powers. In Figures 4 and 5, the red line indicates the feedforward trajectories (where no feedback controller is employed) and the black line designates the target. The blue line shows the system response using a continuous MPC operated on a hypothetically continuous NBI, while the pink line represents the MPC performance on a realistic NBI using PWM. Finally, the green line indicates the hybrid MPC response. The hybrid MPC achieves the target q-profile and W with minimal error while the target is rapidly changing in time and when it is relatively constant, indicating it's effectiveness throughout a tokamak shot. The conventional

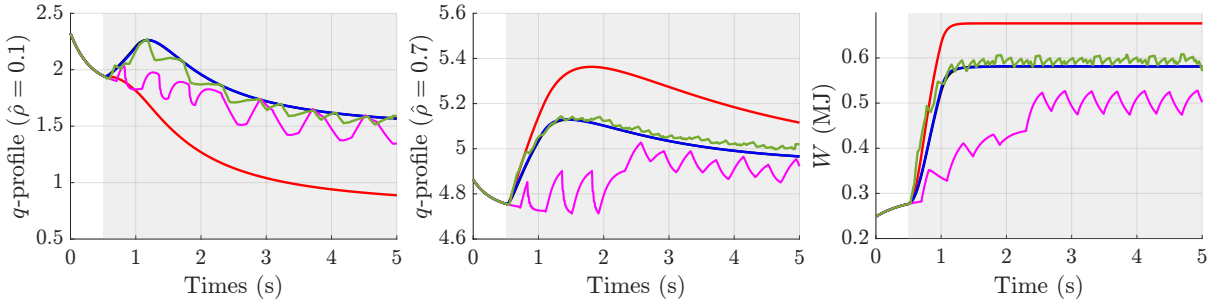

FIG. 4. *Time evolution of the safety factor at $\hat{\rho} = 0.1$ and $\hat{\rho} = 0.5$, and the stored energy for the non-controlled case (red), target (black), conventional MPC without PWM (blue), conventional MPC with PWM (pink), and hybrid MPC (green).*

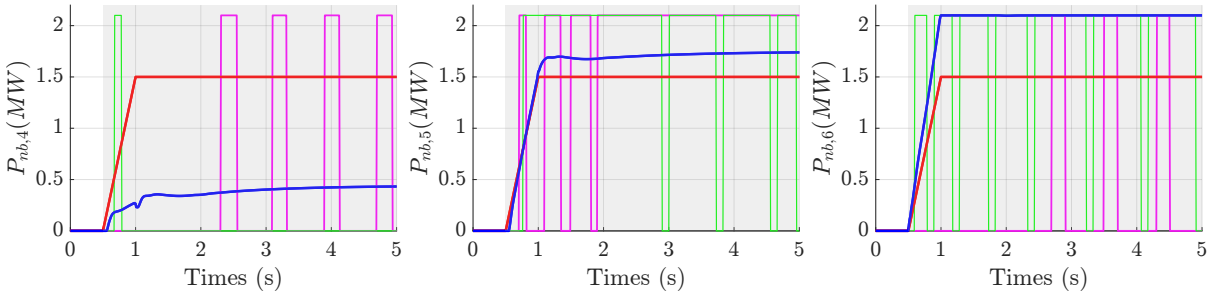

FIG. 5. *NBI power evolutions for the non-controlled case (red), conventional MPC without PWM (blue), conventional MPC with PWM (pink), and hybrid MPC (green).*

MPC is able to follow the target with almost no error. However, once PWM is applied, the conventional MPC is noticeably less effective, having a delayed response to the target and in some cases exhibiting steady state error. Additionally, the conventional MPC+PWM has significant oscillatory behavior, which is greatly reduced by the hybrid MPC. The performance of this conventional MPC+PWM approach is highly sensitive to the constraints assumed for the PWM algorithm. Overall, the hybrid MPC demonstrates that it is able to reach both targets, and has noticeably improved performance compared to a conventional MPC after the PWM conversion.

7. CONCLUSIONS AND FUTURE WORK

A hybrid MPC scheme was developed to regulate the safety factor profile and stored energy. The proposed MPC improves upon the traditional MPC schemes by incorporating discrete constraints that account for the boolean nature of the neutral beam injectors into the problem formulation. These discrete constraints required new techniques to be developed to determine the optimal inputs. In simulation testing on an NSTX-U scenario using COTSIM, the hybrid MPC demonstrated significant improvement over a traditional continous MPC once pulse-width modulation was applied. Future work can include simulation testing on a version of COTSIM that incorporates more plasma dynamics such as a time-varying plasma equilibrium and the addition of a neural-network surrogate model for MMM to model the anomalous diffusivities. Additionally, the hybrid MPC can be expanded to include the plasma current as an input. Furthermore, other optimization techniques for hybrid systems such as cutting plane methods or multiparametric programming can be pursued to potentially improve the optimization process or move the bulk of the computation offline. This could enable lengthening the control horizon. Finally, this hybrid MPC scheme could be modified to control other plasma profiles such as the rotation profile or temperature profile.

ACKNOWLEDGEMENTS

This material is based upon work supported by the U.S. Department of Energy, Office of Science, Office of Fusion Energy under Award Number DE-SC0021385.

DISCLAIMER

apparatus, product, or process disclosed, or represents that its use would not infringe privately owned rights. Reference herein to any specific commercial product, process, or service by trade name, trademark, manufacturer, or otherwise, does not necessarily constitute or imply its endorsement, recommendation, or favoring by the US Government or any agency thereof. The views and opinions of authors expressed herein do not necessarily state or reflect those of the US Government or any agency thereof.

REFERENCES

[1] PAJARES, A. SCHUSTER, E., Current profile and normalized beta control via feedback linearization and Lyapunov techniques, Nuclear Fusion **61** (2021) 036006.

[2] ILHAN, Z. O., BOYER, M. D., SCHUSTER, E., TRANSP-based closed-loop simulations of current profile optimal regulation in NSTX-Upgrade, SI:SOFT-30 **146** (2019) 555.

[3] WANG, S., WITRANT, E., MOREAU, D., Robust control of q-profile and β_p using data-driven models on EAST, Fusion Engineering and Design **162** (2021) 112071.

[4] WANG, H. SCHUSTER, E., Robust control of the current profile and plasma energy in EAST, SI:SOFT-30 **146** (2019) 688.

[5] G. Tartaglione, M. Ariola, W. Bie, et al., Plasma magnetic control for DEMO tokamak using MPC, in *2022 IEEE Conference on Control Technology and Applications (CCTA)*, pp. 825–830, 23.

[6] BOSMAN, T. O. S. J., VAN BERKEL, M., DE BAAR, M. R., Model-based electron density profile estimation and control, applied to ITER, Journal of Physics Communications **5** (2021) 115015.

[7] Z. Wang, H. Wang, E. Schuster, et al., Implementation and Initial Testing of a Model Predictive Controller for Safety Factor Profile and Energy Regulation in the EAST Tokamak, in *2023 American Control Conference (ACC)*, pp. 3276–3281, 2023.

[8] MALJAARS, E., FELICI, F., de Baar, M., et al., Control of the tokamak safety factor profile with time-varying constraints using MPC, Nuclear Fusion **55** (2015) 023001.

[9] Y. Ou E. Schuster, Model predictive control of parabolic PDE systems with dirichlet boundary conditions via Galerkin model reduction, in *2009 American Control Conference*, pp. 1–7, 2009.

[10] MALJAARS, B., FELICI, F., de Baar, M., STEINBUCH, M., Model Predictive Control of the Current Density Distribution and Stored Energy in Tokamak Fusion Experiments using Trajectory Linearizations., 5th IFAC Conference on Nonlinear Model Predictive Control NMPC 2015 **48** (2015) 314.

[11] ILHAN, Z. O., WEHNER, W. P., SCHUSTER, E., Model predictive control with integral action for the rotational transform profile tracking in NSTX-U, in *2016 IEEE Conference on Control Applications (CCA)*, pp. 623–628, Buenos Aires, Argentina, 2016, IEEE.

[12] BEMPORAD, A. MORARI, M., Control of systems integrating logic, dynamics, and constraints, Automatica **35** (1999) 407.

[13] CAMACHO, E., RAMIREZ, D., LIMON, D., MUÑOZ DE LA PEÑA, D., ALAMO, T., Model predictive control techniques for hybrid systems, Annual Reviews in Control **34** (2010) 21.

[14] BALBIS, L., ORDYS, A. W., GRIMBLE, M. J., PANG, Y., Tutorial introduction to the modelling and control of hybrid systems, International Journal of Modelling, Identification and Control **2** (2007) 259.

[15] SUN, X., YUAN, C., CAI, Y., WANG, S., CHEN, L., Model predictive control of an air suspension system with damping multi-mode switching damper based on hybrid model, Mechanical Systems and Signal Processing **94** (2017) 94.

[16] KHAKIMOVA, A., KUSATAYEVA, A., SHAMSHIMOVA, A., et al., Optimal energy management of a small-size building via hybrid model predictive control, Energy and Buildings **140** (2017) 1.

[17] C. A. Orrico, M. van Berkel, T. O. S. J. Bosman, W. P. M. H. Heemels, D. Krishnamoorthy, Mixed-Integer MPC Strategies for Fueling and Density Control in Fusion Tokamaks, IEEE Control Systems Letters **7** (2023) 1897.

[18] YANG, L., KHAWALDEH, H. A., PARUCHURI, S. T., et al., Towards Density Profile Regulation Via Pellet Injection in Tokamaks Using Hybrid Model Predictive Control.

[19] HINTON, F. L. HAZELTINE, R. D., Theory of plasma transport in toroidal confinement systems, Rev. Mod. Phys. **48** (1976) 239.

[20] BARTON, J., BOYER, M., SHI, W., et al., Physics-model-based nonlinear actuator trajectory optimization and safety factor profile feedback control for advanced scenario development in DIII-D, Nuclear Fusion **55** (2015) 093005.

[21] WANG, H., *Model-Based Control of the Current Density Profile in the Experimental Advanced Superconducting Tokamak (EAST)*, PhD thesis, Lehigh University, Ann Arbor, 2019.

[22] ITER Physics Expert Group on Confinement and Transport and ITER Physics Expert Group on Confinement Modelling and Database and ITER Physics Basis Editors, Chapter 2: Plasma confinement and transport, Nuclear Fusion **39** (1999) 2175.